Immunology and Transfusion Medicine for supplying blood components. Sequence data for *P. falciparum* chromosome 13 were obtained from the Sanger Centre (available at www.sanger.ac.uk/Projects/P_falciparum/). Sequencing of *P. falciparum* chromosome 13 was accomplished as part of the Malaria Genome Project, with support by the Wellcome Trust. Preliminary sequence data for *P. falciparum* chromosome 14 were obtained from TIGR (available at www.tigr.org). Sequencing of chromosome 14 was part of the international Malaria Genome Sequencing Project and was supported by awards from the Burroughs Wellcome Fund and the U.S. Department of Defense.

21 April 1999; accepted 29 July 1999

Functional Interaction of BRCA1-Associated BARD1 with Polyadenylation Factor CstF-50

Frida E. Kleiman and James L. Manley*

Polyadenylation of messenger RNA precursors requires a complex protein machinery that is closely integrated with the even more complex transcriptional apparatus. Here a polyadenylation factor, CstF-50 (cleavage stimulation factor), is shown to interact in vitro and in intact cells with a nuclear protein of previously unknown function, BRCA1-associated RING domain protein (BARD1). The BARD1-CstF-50 interaction inhibits polyadenylation in vitro. BARD1, like CstF-50, also interacts with RNA polymerase II. These results indicate that BARD1-mediated inhibition of polyadenylation may prevent inappropriate RNA processing during transcription, perhaps at sites of DNA repair, and they reveal an unanticipated integration of diverse nuclear events.

Almost all eukaryotic mRNAs have a polyadenylated [poly(A)] tail at the 3′ end. Formation of this structure involves endonucleolytic cleavage of the mRNA precursor coupled with poly(A) synthesis, a reaction that requires a complex set of protein factors (*1*). Although polyadenylation can be reconstituted in vitro with purified components and a synthetic mRNA precursor, considerable evidence now exists that, in the cell nucleus, 3′ end formation is normally tightly coupled to transcription by RNA polymerase II (RNAP II). Polyadenylation factors associate with RNAP II at the promoter (*2*) and appear to remain with it during elongation (*3*). When RNAP II reaches the site of polyadenylation, it participates directly in the processing reaction together with the other polyadenylation factors (*4*); it also receives a signal needed for subsequent transcription termination (*5*). How these complex interactions are orchestrated is not known. However, polyadenylation can be regulated, for example, during the cell cycle (*6*) and cellular differentiation (*7*).

Cleavage stimulation factor (CstF) is a polyadenylation factor that helps specify the site of processing (*8, 9*). It is a heterotrimeric protein with subunits of 77, 64, and 50 kD (CstF-77, -64, and -50) that recognizes the G+U–rich element, a sequence located downstream of the cleavage site. RNA binding is mediated by CstF-64 (*10*). CstF-77, or Suppressor-of-forked in *Drosophila*, bridges CstF-64 and -50 (*11*) and interacts with another multisubunit factor, the AAUAAA-binding cleavage-polyadenylation specificity factor (CPSF), to define the poly(A) site (*12*). CstF-50 contains seven WD-40 repeats (*13*), is required for CstF activity in vitro (*11*), and interacts with the COOH-terminal domain of the RNAP II largest subunit (CTD) (*3*).

To identify additional CstF-50–interacting proteins, we performed a yeast two-hybrid assay (*14*); for bait we used CstF-50 fused to the LexA DNA binding domain (*15*). Among the strongest interacters recovered was BARD1 (*16*), a protein known to associate with the breast cancer–associated tumor suppressor BRCA1 in vivo. Both BARD1 and BRCA1 possess NH_2-terminal RING motifs and COOH-terminal BRCT domains, with the former responsible for the BARD1-BRCA1 interaction (*17*). Although the function of BARD1 is unknown, inhibiting its expression in cultured cells results in changes that suggest a premalignant phenotype (*18*). BARD1 likely plays a role in BRCA1-mediated tumor suppression and may itself be a target for tumorigenic mutations in some cancers (*19*). BARD1, in association with BRCA1, can colocalize with the DNA replication and repair factors PCNA and Rad51, perhaps participating in the cellular response to DNA damage (*20*).

The BARD1 cDNAs obtained from the two-hybrid screen encoded amino acids 457 to 777 (Fig. 1A), which includes two of three ankyrin repeats and the BRCT domain. We used essentially full-length BARD1 (amino acid residues 13 to 777), which interacted as efficiently as the smaller fragment, to confirm the interaction in yeast. CstF-50 (amino acid residues 92 to 431), which lacks the NH_2-terminal region of CstF-50, also interacted strongly with BARD1. As observed with BRCA1 (*21*), yeast strains expressing BARD1 displayed a slow-growth phenotype (*22*).

We next characterized the BARD1–CstF-50 interaction in vitro. The two proteins were translated separately in vitro, mixed, and subjected to immunoprecipitation with antibodies to BARD1 (anti-BARD1 antibodies) (*23*) (Fig. 2A). CstF-50 was precipitated in the presence (lane 3), but not in the absence (lane 2), of BARD1, which strongly suggests a specific interaction between the two proteins. In another approach, a glutathione S-transferase (GST)–BARD1 fusion protein (BARD1 residues 13 to 777) was purified from *Escherichia coli* and used in protein interaction assays, again with in vitro translated CstF-50 (Fig. 2B). A significant fraction of the input CstF-50 bound to GST-BARD1 (lane 3) but not to GST alone (lane 2). COOH-terminal truncations of CstF-50 (see Fig. 1B) eliminated binding (lanes 4 to 7), consistent with the requirement of at least the seventh WD-40 repeat for interaction. To elucidate the region of BARD1 required, we used additional GST-BARD1 derivatives (Fig. 1B) in binding assays with CstF-50 (Fig. 2C). A COOH-terminal truncation removing most of

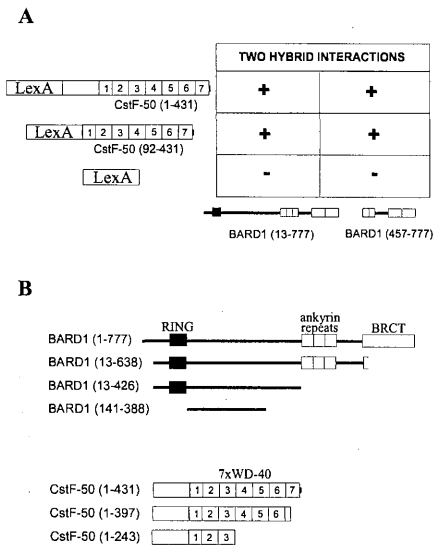

Fig. 1. Interaction of BARD1 and CstF-50 in yeast. **(A)** Two-hybrid screening identifies a CstF50–BARD1 interaction. LexA–CstF50 fusion proteins are indicated on the left and BARD1 derivatives are shown below. Features of proteins are indicated and numbers represent amino acid residue. Interactions were detected by LEU2 and LacZ expression. **(B)** Diagram of BARD1 and CstF-50 derivatives used in in vitro experiments. Proteins were produced by in vitro translation or as NH_2-terminal GST fusions in *E. coli*.

Department of Biological Sciences, Columbia University, New York, NY 10027, USA.

*To whom correspondence should be addressed. E-mail: jlm2@columbia.edu

the BRCT domain only slightly reduced binding (compare lanes 3 and 4), indicating that this region is not essential. However, two different derivatives lacking the ankyrin repeats failed to bind CstF-50 (lanes 5 and 6). In combination, the data suggest that the two COOH-terminal ankyrin repeats, the region just downstream, or both constitute the CstF-50 interaction domain.

To determine whether CstF-50 interacts with BARD1 in vivo, we analyzed HeLa cell nuclear extracts (NE) by cofractionation and coimmunoprecipitation (*24*). Because CstF-50 is part of the CstF heterotrimer, we used an antibody directed against another subunit, CstF-64, which ensured that any interactions detected were with intact CstF. We first tested whether the proteins could be coimmunoprecipitated from NE. The results (Fig. 3A) indicate that antibodies against either protein coprecipitated a small but significant fraction of the other, as judged by immunoblots of the immunoprecipitates (IPs) (lanes 1 to 5). Extraneous antibodies did not immunoprecipitate either protein (lanes 6 and 7), nor did either antibody cross-react with the other protein (*22*). We also followed the proteins during the early steps of CstF purification, which includes $(NH_4)_2SO_4$ fractionation followed by Superose-6 gel filtration (*25*). This produces a fraction, cleavage-specificity factor (CSF), that contains all the factors essential for 3′ cleavage. Immunoblotting of the Superose fractions (Fig. 3B) revealed, as expected, significant amounts of CstF coeluting with CSF activity. However, large amounts were also detected in more rapidly eluting fractions. BARD1, on the other hand, was found predominantly in the heavier fractions, with smaller amounts in the CSF active fractions. To determine whether BARD1 and CstF were associated in these fractions, we again performed coimmunoprecipitation experiments. Given the interaction between BARD1 and BRCA1 (*16, 20*), we also examined the possible presence of BRCA1 in CstF-containing complexes. We obtained similar results with all fractions that contained the three proteins; Fig. 3C presents results obtained with fraction 22. Strikingly, all three antibodies precipitated not only their cognate protein but also significant amounts of the other two. These findings indicate that the CstF50-BARD1 interaction occurs in the nuclei of HeLa cells and is likely to be physiologically relevant.

We next determined whether BARD1 affects polyadenylation in vitro. During preliminary experiments aimed at developing conditions for immunodepletion of NE, we observed that the cleavage step was enhanced by addition of an anti-BARD1 monoclonal antibody (mAb), EE6 (*16*), and we developed conditions that allowed this activation to be observed reproducibly (*26*) (Fig. 4A). We monitored cleavage of a simian virus 40 late pre-mRNA substrate in a limiting amount of NE that had been preincubated with no additions (lane 1) or with increasing amounts of anti-BARD1 (lanes 2 to 4) or anti-p53 (lanes 5 to 7). The anti-BARD1 mAb significantly and specifically enhanced cleavage, which suggests that BARD1 may antagonize 3′ end formation. Inclusion of increasing amounts of purified GST-BARD1 in the preincubation mixture prevented antibody activation and

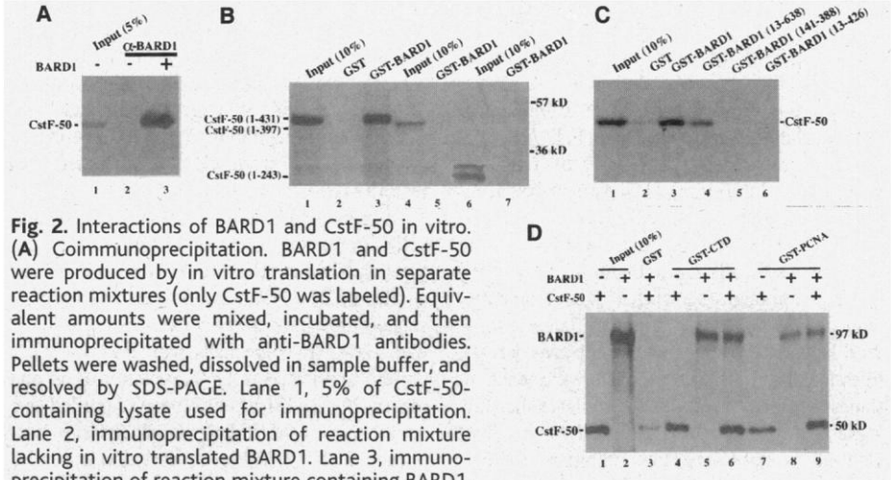

Fig. 2. Interactions of BARD1 and CstF-50 in vitro. (**A**) Coimmunoprecipitation. BARD1 and CstF-50 were produced by in vitro translation in separate reaction mixtures (only CstF-50 was labeled). Equivalent amounts were mixed, incubated, and then immunoprecipitated with anti-BARD1 antibodies. Pellets were washed, dissolved in sample buffer, and resolved by SDS-PAGE. Lane 1, 5% of CstF-50-containing lysate used for immunoprecipitation. Lane 2, immunoprecipitation of reaction mixture lacking in vitro translated BARD1. Lane 3, immunoprecipitation of reaction mixture containing BARD1. (**B**) Interaction of GST-BARD1 and CstF-50. Full-length CstF-50 (lanes 1 to 3) and the two indicated COOH-terminal truncations (lanes 4 to 7) were produced by in vitro translation and incubated with purified GST (lane 2) or GST-BARD1 (lanes 3, 5, and 7). Bound proteins were eluted and resolved by SDS-PAGE. Ten percent of each of the CstF-50 derivatives used in binding reactions is shown in lanes 1, 4, and 6. (**C**) Requirement of BARD1 ankyrin repeats for CstF-50 interaction. GST (lane 2) and the indicated GST-BARD1 derivatives (lanes 3 to 6) were used in in vitro binding reactions with full-length CstF-50 produced by in vitro translation. Lane 1 contains 10% of the CstF-50 used in binding reactions. (**D**) Interaction with RNAP II CTD and with PCNA. BARD1 and CstF-50 were produced by in vitro translation (lanes 1 and 2) and incubated with 1 μg of either GST (lane 3), GST-CTD (lanes 4 to 6), or GST-PCNA (lanes 7 to 9). Binding reactions were performed and analyzed as in (B).

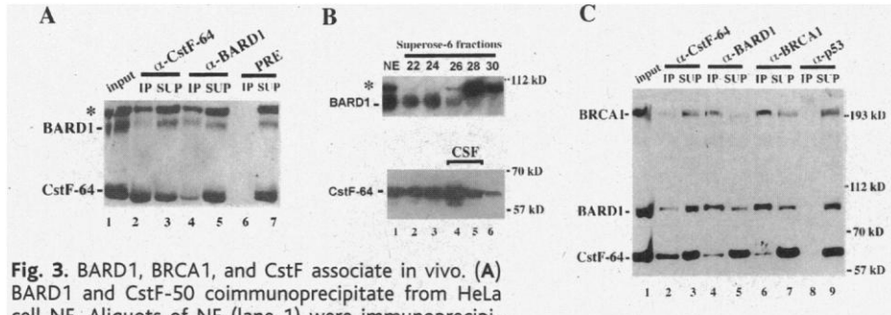

Fig. 3. BARD1, BRCA1, and CstF associate in vivo. (**A**) BARD1 and CstF-50 coimmunoprecipitate from HeLa cell NE. Aliquots of NE (lane 1) were immunoprecipitated with anti-CstF64 (lanes 2 and 3), anti-BARD1 (lanes 4 and 5) or preimmune (lanes 6 and 7) antibodies. Equivalent amounts of the pellets (IP; lanes 2, 4, and 6) and supernatants (SUP; lanes 3, 5, and 7) were resolved by SDS-PAGE and proteins were detected by immunoblotting with anti-BARD1 or CstF-64 antibodies. Positions of BARD1 and CstF-64 are indicated. Asterisk indicates a species detected by the anti-BARD1 mAb. It can be separated from authentic BARD1 [see (B)], and its relationship to BARD1 is currently unknown (*35*). However, the fact that it can be coimmunoprecipitated not only with the anti-BARD1 polyclonal but also with the anti-CstF64 mAb and the anti-BRCA1 mAb (*22*) strongly suggests that it is related to BARD1. (**B**) Cofractionation of BARD1 and CstF. NE was subjected to 20% to 40% ammonium sulfate fractionation and Superose-6 gel filtration. Aliquots from NE and fractions 22 to 30 of the column were resolved by SDS-PAGE, and proteins were detected by immunoblotting with anti-BARD1 and anti-CstF64 antibodies. Positions of BARD1 and CstF-64 are indicated. Asterisk denotes the putative BARD1-related species [see (A)]. CSF activity was present in fractions 26 to 28. (**C**) Association of CstF, BARD1, and BRCA1 in a high molecular weight Superose-6 fraction. Aliquots of a fraction equivalent to fraction 22 in (B) were subjected to immunoprecipitation exactly as in (A), except that an anti-BRCA1 antibody was used in both the immunoprecipitation and immunoblotting (lanes 6 and 7) in addition to the anti-BARD1 (lanes 4 and 5) and anti-CstF64 (lanes 2 and 3) antibodies. An anti-p53 mAb was used as an irrelevant control (lanes 8 and 9). Positions of proteins are indicated on the left and sizes are on the right.

completely inhibited cleavage at the highest concentrations (Fig. 4B, lanes 1 to 5). GST-BARD1 also was sufficient to block cleavage (Fig. 4C, lanes 1 to 4). Essentially identical results, with both antibody activation and inhibition by GST-BARD1, were observed with a second pre-mRNA, adenovirus L3 (*22*). These results indicate that BARD1 inhibits the first step of mRNA 3′ end formation in vitro and may explain why the active CSF fractions from the Superose column contained relatively little BARD1 (Fig. 3B).

We next examined regions of BARD1 required for inhibition. The results, shown in Fig. 4D, correlate well with the binding data in Fig. 2C. GST-BARD1 (residues 13 to 638), which lacks the BRCT domain, inhibited processing, although somewhat less efficiently than did GST-BARD1 (compare lanes 2 to 4 with lanes 5 to 7). In contrast, the two derivatives lacking the ankyrin repeats were inactive (lanes 8 to 13). These results indicate that the same region of BARD1 required for binding CstF-50 is necessary for inhibiting 3′ pre-mRNA cleavage.

We suggest two related models in which the in vivo function of BARD1 is to prevent premature or incorrect 3′ end formation. The first stems from the previously documented interaction of CstF, as well as BRCA1, with the RNAP II holoenzyme (*3, 27*). The tight association between BRCA1 and BARD1 suggests that BARD1 may also be associated with RNAP II. Indeed, we found that in vitro translated BARD1 bound to a GST-CTD fusion protein with the same efficiency as CstF-50 (Fig. 2D, lanes 4 to 6) (*3*). BRCA1, in contrast, did not bind GST-CTD (*22*), and it is conceivable that the BARD1-CTD interaction contributes to the presence of BRCA1 in the holoenzyme. Our data suggest that, because of BARD1, the polyadenylation apparatus associated with the holoenzyme is inactive, which would prevent inappropriate processing of nascent transcripts—for example, at sites of RNAP II pausing or at cryptic or pseudo-poly(A) signals within the body of the transcript. By this view, the absence of BARD1 could lead to prematurely terminated transcripts and production of truncated, potentially deleterious proteins.

A related possibility is that BARD1 prevents premature polyadenylation of nascent transcripts associated with polymerases stalled at sites of DNA damage. Several observations support this hypothesis. First, BRCA1, likely with BARD1, colocalizes with Rad51 (*28*), a protein implicated in DNA recombination and repair (*29*). Rad51 has also been identified as a component of the RNAP II holoenzyme, supporting the link between transcription and DNA repair (*30*); genetic studies have also implicated BRCA1 in transcription-coupled repair of oxidative DNA damage (*31*). Second, BRCA1, BARD1, and Rad51 colocalize with the DNA replication and repair factor PCNA to sites of DNA damage during S phase (*20*). Remarkably, the strongest CstF-50–interacting protein isolated in our two-hybrid screen was PCNA (*22*). The interaction required the CstF-50 NH_2-terminus, which contains a sequence similar to the consensus PCNA interaction motif (*32*), and was observed in vitro with GST-PCNA and in vitro translated CstF-50 (Fig. 2D, lanes 7 to 9; these data also show an interaction between BARD1 and PCNA, consistent with their known colocalization). Together, these results suggest a model in which BARD1, as part of the RNAP II holoenzyme, senses sites of DNA damage and repair, and the inhibitory interaction with CstF ensures that nascent RNAs are not erroneously polyadenylated at such sites.

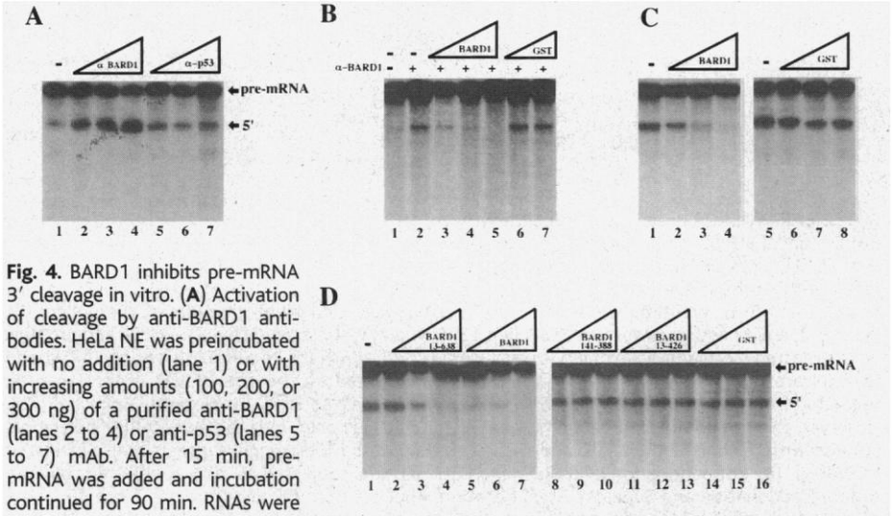

Fig. 4. BARD1 inhibits pre-mRNA 3′ cleavage in vitro. (**A**) Activation of cleavage by anti-BARD1 antibodies. HeLa NE was preincubated with no addition (lane 1) or with increasing amounts (100, 200, or 300 ng) of a purified anti-BARD1 (lanes 2 to 4) or anti-p53 (lanes 5 to 7) mAb. After 15 min, pre-mRNA was added and incubation continued for 90 min. RNAs were purified and analyzed by denaturing PAGE. Positions of pre-mRNA and the 5′ cleavage product are indicated. (**B**) GST-BARD1 reverses activation by anti-BARD1 antibodies. NE was preincubated with no addition (lane 1); with 200 ng of anti-BARD1 (lanes 2 to 8); and with 50, 100, or 200 ng of GST-BARD1 (lanes 3 to 5) or 100 or 200 ng of GST (lanes 6 and 7). Pre-mRNA was added and reaction mixtures were processed as in (A). (**C**) Inhibition of 3′ processing by GST-BARD1. NE was preincubated with no additions (lanes 1 and 5) or with 50, 100, or 150 ng of GST-BARD1 (lanes 2 to 4) or GST (lanes 6 to 8). Pre-mRNA was added and reaction mixtures were processed as in (A). (**D**) Domain requirements for inhibition of 3′ processing by GST-BARD1. Processing reactions were performed as in (C), except that 50, 100, or 150 ng of the indicated GST-BARD1 derivative was used.

References and Notes

1. E. Wahle and W. Keller, *Trends Biochem. Sci.* **21**, 247 (1996); D. F. Colgan and J. L. Manley, *Genes Dev.* **11**, 2755 (1997).
2. J. C. Dantonel, K. G. K. Murthy, J. L. Manley, L. Tora, *Nature* **389**, 399 (1997).
3. S. McCracken *et al.*, *ibid.* **385**, 357 (1997).
4. Y. Hirose and J. L. Manley, *ibid.* **395**, 93 (1998).
5. E. Whitelaw and N. Proudfoot, *EMBO J.* **5**, 2915 (1986); J. Logan, E. Falck-Pedersen, J. E. Darnell, T. Shenk, *Proc. Natl. Acad. Sci. U.S.A.* **84**, 8306 (1987); S. Connelly and J. L. Manley, *Genes Dev.* **2**, 440 (1988).
6. D. F. Colgan, K. G. K. Murthy, C. Prives, J. L. Manley, *Nature* **384**, 282 (1996); D. F. Colgan, K. G. K. Murthy, W. Zhao, C. Prives, J. L. Manley, *EMBO J.* **17**, 1053 (1998).
7. Y. Takagaki, R. L. Seipelt, M. L. Peterson, J. L. Manley, *Cell* **87**, 941 (1996); Y. Takagaki and J. L. Manley, *Mol. Cell* **2**, 761 (1998).
8. Y. Takagaki, L. C. Ryner, J. L. Manley, *Genes Dev.* **3**, 1711 (1989); G. M. Gilmartin and J. R. Nevins, *Mol. Cell. Biol.* **11**, 2432 (1991); K. G. K. Murthy and J. L. Manley, *J. Biol. Chem.* **267**, 14804 (1992).
9. Y. Takagaki, J. L. Manley, C. C. MacDonald, J. Wilusz, T. Shenk, *Genes Dev.* **4**, 2112 (1990).
10. Y. Takagaki, C. C. MacDonald, T. Shenk, J. L. Manley, *Proc. Natl. Acad. Sci. U.S.A.* **89**, 1403 (1992); C. C. MacDonald, J. Wilusz, T. Shenk, *Mol. Cell. Biol.* **14**, 6647 (1994); K. Beyer, T. Dandekar, W. Keller, *J. Biol. Chem.* **272**, 26769 (1997); Y. Takagaki and J. L. Manley, *Mol. Cell. Biol.* **17**, 3907 (1997).
11. Y. Takagaki and J. L. Manley, *Nature* **372**, 471 (1994).
12. K. G. K. Murthy and J. L. Manley, *Genes Dev.* **9**, 2672 (1995).
13. Y. Takagaki and J. L. Manley, *J. Biol. Chem.* **267**, 23471 (1992).
14. J. Gyuris, E. Golemis, H. Chertkov, R. Brent, *Cell* **75**, 791 (1993).
15. Yeast interaction trap selection assays were performed as in (*14*). Bait plasmids were constructed by insertion of polymerase chain reaction amplified fragments into LexA(202+pl). A cDNA library from human fetal brain RNA was screened. Library plasmids from positive colonies were rescued, used to transform *Escherichia coli*, and sequenced. Specificity was confirmed with several other LexA fusion proteins. Although LexA–CstF-50 plus BARD1-B42 again resulted in reporter gene expression, no other combination tested resulted in detectable activity (*22*).
16. L. C. Wu *et al.*, *Nature Genet.* **14**, 430 (1996).
17. T. C. Ayi, J. T. Tsan, L. Y. Hwang, A. M. Bowcock, R. Baer, *Oncogene* **17**, 2143 (1998); J. E. Meza, P. S. Brzovic, M. C. King, R. E. Klevit, *J. Biol. Chem.* **274**, 5659 (1999).
18. I. Irminger-Finger, J. V. Soriano, G. Vaudan, R. Montesano, A. P. Sappino, *J. Cell. Biol.* **143**, 1329 (1998).
19. T. H. Thai *et al.*, *Hum. Mol. Genet.* **7**, 195 (1998).
20. R. Scully *et al.*, *Cell* **90**, 425 (1997); Y. Jin *et al.*, *Proc. Natl. Acad. Sci. U.S.A.* **94**, 12075 (1997).
21. J. S. Humphrey *et al.*, *Proc. Natl. Acad. Sci. U.S.A.* **94**, 5820 (1997).
22. F. E. Kleiman and J. L. Manley, unpublished data.
23. CstF-50 and BARD1 were generated by in vitro translation in rabbit reticulocyte lysate. Six microliters of the CstF-50 lysate was incubated with or without 6 μl of the BARD1 lysate for 30 min at 30°C in buffer A (final volume, 20 μl; 1× phosphate-buffered saline (137 mM NaCl, 3 mM KCl, 10 mM Na_2HPO_4, 1.8 mM KH_2PO_4, 0.01% Nonidet P-40, 0.04% bovine serum albumin). BARD1-specific polyclonal antibodies (383D) (*16*) were coupled to protein A–Sepharose beads and, after washing, binding mixtures were incubated with

the beads for 90 min at 4°C, washed four times with buffer B (buffer A plus 100 mM NaCl), resuspended in loading buffer, and fractionated by SDS–8% polyacrylamide gel electrophoresis (PAGE). For GST fusion protein interaction assays, cDNAs encoding full-length or truncated BARD1 were inserted into pGEX-2TK and expressed in *E. coli*. Proteins were purified by binding to and eluting from glutathione-agarose beads, and 1 mg of the indicated protein was incubated with ^{35}S-labeled CstF-50. Conditions were as in the coimmunoprecipitation assays, except washing was with buffer B containing 300 mM NaCl.

24. HeLa cell NE was subjected to a 20% to 40% $(NH_4)_2SO_4$ cut and fractionated by Superose-6 chromatography (*25*). Selected fractions were analyzed by immunoblotting with mAbs targeted against BARD1 (EE 6) (*16*), CstF-64 (*9*), or BRCA1 (MS110) (*33*). NE and fractions eluting from Superose-6 were immunoprecipitated with the anti-BARD1 polyclonal antibody, or the anti-CstF64 or BRCA1 mAbs, bound to protein A–Sepharose beads. Immunoprecipitations were carried out in buffer B at 4°C for 90 min, and washing was with buffer B. Aliquots of pellets and supernatants were analyzed by SDS-PAGE and immunoblotting. The anti-BARD1 and CstF-64 antibodies did not cross-react with CstF-64 and BARD1, respectively, as judged by experiments with purified (BARD1-free) CstF and recombinant GST–BARD1 (*22*).
25. Y. Takagaki, L. C. Ryner, J. L. Manley, *Cell* **52**, 731 (1988).
26. ^{32}P-labeled pre-mRNA substrates were prepared as in (*34*). Cleavage assays in NE were carried out in reaction mixtures containing 0.2 to 0.5 ng of labeled RNA, 250 ng of tRNA, 0.25 unit of RNasin (Promega), 9.6 mM Hepes·NaOH (pH 7.9), 9.6% glycerol, 24 mM $(NH_4)_2SO_4$, 20 mM creatine phosphate, 0.24 mM dithiothreitol, 2.5% polyvinyl alcohol, 0.24 mM phenylmethylsulfonyl fluoride, and either 2 mM EDTA or 1 mM $MgCl_2$. NE and added proteins or antibodies were preincubated for 15 min at 30°C, after which the pre-mRNA was added and incubation continued for an additional 90 min. RNA products were isolated and fractionated on 5% polyacrylamide, 8.3 M urea gels.
27. R. Scully *et al.*, *Proc. Natl. Acad. Sci. U.S.A.* **94**, 5605 (1997).
28. R. Scully *et al.*, *Cell* **88**, 265 (1997).
29. A. Shinohara, H. Ogawa, T. Ogawa, *Cell* **69**, 457 (1992); P. Baumann, F. E. Benson, S. C. West, *ibid.* **87**, 757 (1996).
30. E. Maldonado *et al.*, *Nature* **381**, 86 (1996).
31. L. C. Gowen *et al.*, *Science* **281**, 1009 (1998).
32. E. Warbrick, W. Heatherington, D. P. Lane, D. M. Glover, *Nucleic Acids Res.* **26**, 3925 (1998).
33. R. Scully *et al.*, *Science* **272**, 123 (1996).
34. Y. Hirose and J. L. Manley, *J. Biol. Chem.* **272**, 29636 (1997).
35. J. Chen, D. Livingston, R. Baer, personal communication.
36. Supported by National Institutes of Health (NIH) grant GM28983 to J.L.M. and an NIH Fogarty Fellowship to F.E.K. We thank Y. Takagaki for CstF plasmids and antibodies; R. Baer for BARD1 and BRCA1 encoding plasmids and anti-BARD1 antibodies; J. Chen and D. Livingston for the anti-BRCA1 antibody; R. Brent for yeast two-hybrid reagents; Y. Hirose for HeLa nuclear extract; and C. Prives, R. Baer, Y. Hirose, and R. Tacke for advice and discussions.

25 June 1999; accepted 29 July 1999

Control of Circadian Rhythms and Photoperiodic Flowering by the *Arabidopsis GIGANTEA* Gene

Deok Hoon Park,[1]* David E. Somers,[2]* Yang Suk Kim,[1] Yoon Hi Choy,[1] Hee Kyun Lim,[1] Moon Soo Soh,[1] Hyo Jung Kim,[1] Steve A. Kay,[2] Hong Gil Nam[1]†

Photoperiodic responses in plants include flowering that is day-length–dependent. Mutations in the *Arabidopsis thaliana GIGANTEA* (*GI*) gene cause photoperiod-insensitive flowering and alteration of circadian rhythms. The *GI* gene encodes a protein containing six putative transmembrane domains. Circadian expression patterns of the *GI* gene and the clock-associated genes, *LHY* and *CCA1*, are altered in *gi* mutants, showing that GI is required for maintaining circadian amplitude and appropriate period length of these genes. The *gi-1* mutation also affects light signaling to the clock, which suggests that GI participates in a feedback loop of the plant circadian system.

The circadian clock system is a self-sustained biological oscillator with a period of ~24 hours that operates ubiquitously in animals, plants, and microorganisms (*1, 2*) and controls a wide range of rhythmic processes (*3, 4*). In plants, the circadian clock controls daily changes of photosynthetic activities, leaflet movement, cell growth, and expression of several genes, including the chlorophyll a/b binding protein (*CAB*) genes (*2, 5*). Several components regulating the circadian system have been genetically defined in *Arabidopsis thaliana* (*6, 7*). However, molecular components controlling the plant circadian system are largely unknown, except for the two clock-associated factors, LHY and CCA1 (*8, 9*).

The ability to perceive changes in day length (*7, 10–12*), photoperiodism, is essential for organisms to recognize seasonal changes and is associated with the circadian clock system (*4, 7–9*). *Arabidopsis* is a facultative long-day plant, flowering in a fewer number of days under long photoperiods than under short photoperiods. Certain alleles of the *Arabidopsis gi* mutants are insensitive to photoperiod (*11, 13, 14*). Here, we report an important role for GI in plant circadian function and molecular nature of the *Arabidopsis gi* mutations.

Cotyledons and leaves of *Arabidopsis* show circadian movement, rising and falling in relative position during subjective night and day, respectively (*7*). Measurement of leaf movement rhythms (*15*) revealed that both the *gi-1* and *gi-2* mutants have shorter circadian periods than wild-type plants (Fig. 1, A and B, and Table 1).

Expression of the *CAB2* gene is under the control of the circadian clock in *Arabidopsis*. To characterize the effects of the *gi* mutations on the circadian system, we crossed the clock-controlled reporter construct, *cab2::luciferase* (*cab2::luc*) (*6*), into the *gi-1* and *gi-2* backgrounds. Both mutants alter the circadian period of *cab2::luc* expression (Fig. 1C and Table 1) (*15*). The period is substantially shorter in the homozygous *gi-1* mutant than in the wild type, and this effect is dependent on gene dosage (Fig. 2A and Table 1). In contrast, the *gi-2* mutation causes the period to lengthen and is fully recessive (Fig. 2B and Table 1). Luminescence cycling in the *gi-2* background remained in phase with the wild type for up to 60 hours after transfer to continuous white light (LL), after which the period lengthened (Fig. 1C) (*15, 16*). There was no apparent lag in the period-shortening effects of the *gi-1* mutation (Fig. 1C). Both mutations caused an abnormally rapid damping of rhythm amplitude.

We cloned the *GI* gene with a map-based approach. The *GI* locus is linked to the *THIAMINE REQUIRING 1* (*TH1*) locus on chromosome 1 (*17*). We thus used the *TH1* gene to screen an *A. thaliana* bacterial artificial chromosome (BAC) library, identifying the BAC clone T23L3 (*18*). Subsequent probing with T23L3 identified two contiguous BAC clones, T14K14 and T22J18 (*19*). The *gi-1* and *gi-2* alleles were generated by x-ray mutagenesis (*13*), which frequently generates deletion mutants. When wild-type (Columbia), *gi-1*, and *gi-2* genomic DNA were digested with Stu I and probed with theT22J18 clone, two restriction fragments (7.1 and 1.1 kb, respectively) detected in the wild-type and *gi-2* lines appeared as a single 8.2-kb band in the *gi-1* mutant (*19*). End sequences of the 7.1- and 1.1-kb fragments (*20*) matched a genomic sequence (GenBank accession number Y12227) that contains a predicted open reading frame (ORF) of 1167 amino acids. Sequence comparisons in this region between the wild-type, *gi-1*, and *gi-2* lines revealed small deletions within the predicted ORF in both mutants (*19*).

[1]Department of Life Science, Pohang University of Science and Technology, Pohang, Kyungbuk, 790-784, Korea. [2]Department of Cell Biology and National Science Foundation Center for Biological Timing, The Scripps Research Institute, 10550 North Torrey Pines Road, La Jolla, CA 92307, USA.

*These authors contributed equally to this work.
†To whom correspondence should be addressed. E-mail: hgn@bric.postech.ac.kr